Article

Self-Assembled Monolayers of Electroactive Polychlorotriphenylmethyl Radicals on Au(111)

Núria Crivillers, Marta Mas-Torrent, José Vidal-Gancedo, Jaume Veciana, and Concepció Rovira

J. Am. Chem. Soc., **2008**, 130 (16), 5499-5506 • DOI: 10.1021/ja710845v • Publication Date (Web): 01 April 2008

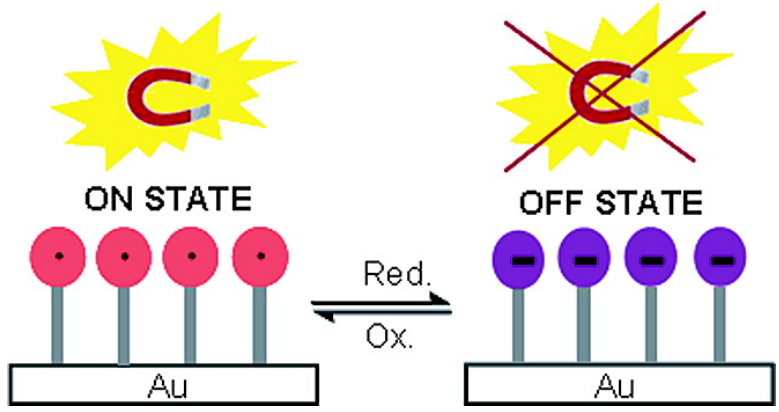

J|A|C|S
ARTICLES

Published on Web 04/01/2008

Self-Assembled Monolayers of Electroactive Polychlorotriphenylmethyl Radicals on Au(111)

Núria Crivillers, Marta Mas-Torrent, José Vidal-Gancedo, Jaume Veciana, and Concepció Rovira*

Institut de Ciència de Materials de Barcelona (CSIC) and Networking Research Center on Bioengineering, Biomaterials and Nanomedicine (CIBER-BBN), Campus Universitari de Bellaterra, 08193 Cerdanyola del Vallès, Spain

Received December 5, 2007; E-mail: cun@icmab.es

Abstract: Two new polychlorotriphenylmethyl (PTM) derivatives bearing a thioacetate and a disulfide group have been synthesized to anchor on gold substrate. On the basis of these molecules, three strategies were followed to prepare self-assembled monolayers (SAMs) of electroactive PTMs. The resulting SAMs were fully characterized by contact angle, atomic force microscopy (AFM), and time-of-flight secondary ion mass spectroscopy (ToF-SIMS). The high coverage surface and stability of the SAMs were demonstrated by cyclic voltammetry. In addition, the electrochemical experiments proved that these SAMs are bistable since it is possible to reversibly switch between the PTM radical state to the corresponding anion. The magnetic response was investigated by electron paramagnetic resonance. We observed that when the PTM SAMs are in their radical form they confer magnetic functionality to the surface, whereas when they are in the anionic state, the surface is diamagnetic. Thus, the PTM-modified substrates are multifunctional surfaces since they combine magnetic and electroactive properties. The reported results show the high potential of these materials for the fabrication of surface molecular devices.

Introduction

In the field of molecular electronics, the utilization of functional molecular building blocks for preparing memory devices has attracted a great deal of interest due to its potential to move toward miniaturization and to fabricate high density data storage devices. For this purpose, it is crucial to control the deposition on surfaces of bistable molecules that can be reversibly magnetically, optically, or electrochemically interconverted between two stable states. In addition, it is required that both states exhibit different responses in order to be able to read the status of the switch. One approach to scale-down to molecular level memory devices is to address single molecule magnets on surfaces since the presence of a large magnetic hysteresis in these systems makes them suitable as molecular components for magnetic information storage.[1] The surface deposition of molecules that can be photochemically converted to a different isomer or derivative is also promising for storing optical data.[2] Another strategy is focused on the fabrication of charge storage devices by substrate immobilization of molecules that can be reversibly oxidized and reduced.[2a,3] A simple and versatile technique to address all these molecular building blocks on surfaces is the preparation of self-assembled monolayers (SAMs),[4] which allows the functionalization of surfaces with a layer of molecules, two-dimensionally organized, that gives to the substrate new properties governed by the inherent characteristics of the molecules adsorbed on it. SAMs have been widely used in molecular electronics[5] and for the design of devices for applications such as sensors[6] or biological arrays.[7]

The preparation of polychlorotriphenylmethyl (PTM) radical SAMs is interesting since they give rise to multifunctional surfaces that combine optical, electrochemical, and magnetic properties. Of particular interest is the deposition of organic radicals on surfaces since they confer the magnetic functionality to the surface. Previously, we have shown that is possible to prepare SAMs of electroactive PTM radicals on silicon oxide and employ them as chemical redox switches with optical (absorption and fluorescence) and magnetic response.[8] In addition to this work, to the best of our knowledge, there are only three other examples in the literature regarding SAMs of

(1) (a) Cornia, A.; Fabretti, A. C.; Pacchioni, M.; Zobbi, L.; Bonacchi, D.; Caneschi, A.; Gatteschi, D.; Biagi, R.; del Pennino, U.; de Renzi, V.; Gurevich, L.; Van der Zan, H. S. J. *Angew. Chem., Int. Ed.* **2003**, *42*, 1645–1648. (b) Ruiz-Molina, D.; Mas-Torrent, M.; Gomez, J.; Balana, A. J.; Domingo, N.; Tejada, J.; Martinez, M. T.; Rovira, C.; Veciana, J. *Adv. Mater.* **2003**, *15*, 42–45.

(2) (a) Namiki, K.; Sakamoto, A.; Murata, M.; Kume, S.; Nishihara, H. *Chem. Commun.* **2007**, 4650–4652. (b) Areephong, J.; Browne, W. R.; Katsonis, N.; Feringa, B. L. *Chem. Commun.* **2006**, 3930–3932. (c) Willner, I. *Acc. Chem. Res.* **1997**, *30*, 347–356.

(3) Shukla, A. D.; Das, A.; van der Boom, M. E. *Angew. Chem., Int. Ed.* **2005**, *44*, 3237–3240.

(4) Love, J. C.; Estroff, L. A.; Kriebel, J. K.; Nuzzo, R. G.; Whitesides, G. M. *Chem. Rev.* **2005**, *105*, 1103–1169.

(5) (a) Flood, A. H.; Stoddart, J. F.; Steureman, D. W.; Heath, J. R. *Science* **2004**, *306*, 2055–2056. (b) Carroll, R. Cl.; Gorman, C. B. *Angew. Chem., Int. Ed.* **2002**, *41*, 4379–4400. (c) Chen, J.; Reed, M. A.; Rawlett, M. A.; Tour, J. M. *Science* **1999**, *286*, 1550–1551. (d) Reed, M. A.; Zhou, C.; Muller, C. J.; Burgin, T. P.; Tour, J. M. *Science* **1997**, *278*, 252–254. (e) Hzp, B.; Akweman, P. W. M.; Blom, D. M.; deLeeuw, B.; de, Boer. *Nature* **2006**, *441*, 69–72.

(6) (a) Crego-Calama, M.; Reinhoudt, D. N. *Adv. Mater.* **2001**, *13*, 1171–1174. (b) Zhang, S.; Cardona, C. M.; Echegoyen, L. *Chem. Commun* **2006**, *43*, 4461–4473.

(7) (a) Pirrung, M. C. *Angew. Chem., Int. Ed.* **2002**, *41*, 1276–1289. (b) Wilson, B. S.; Node, S. *Angew. Chem., Int. Ed.* **2003**, *42*, 494–500.

Scheme 1. Representation of the Three Strategies (*Paths a, b,* and *c*) Carried Out to Obtain the Electroactive PTM SAM

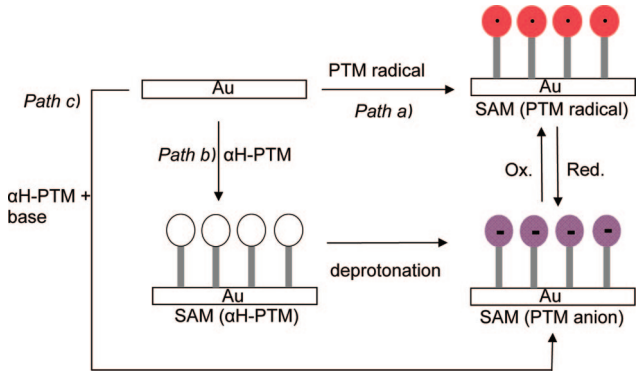

organic radicals, and they are all based on nitronyl nitroxide radicals.[9] PTM radicals offer an attractive alternative since they are chemically and thermally stable due to the fact that their open-shell centers are shielded by six bulky chlorine atoms.[10] Moreover, this family of compounds is electroactive, yielding reversibly the corresponding carboanion (or carbocation) by electrochemical reduction (or oxidation).[11]

Here we describe the adsorption of two newly synthesized PTM derivatives on a gold surface. The magnetic and electrochemical behavior of the resulting SAMs is also demonstrated, showing the potential of these molecular building blocks for preparing multifunctional molecular devices on surfaces.

Results and Discussion

Design of PTM Derivatives for Anchoring on a Au Surface. Three different strategies for the formation of electroactive PTM SAMs on gold have been followed (Scheme 1). *Path a* involves the direct adsorption of a PTM radical species on gold, whereas in *path b*, two steps are required. The first step is based on the formation of a SAM with a protonated precursor of the desired PTM derivative (i.e., αH-PTM), which does not exhibit redox properties. Then, through a base-induced deprotonation reaction, αH-PTM is converted to the corresponding electroactive anion. In the third approach, *path c*, the electroactive SAM is prepared by direct assembling of an anionic PTM species, which is generated from a solution of its αH-PTM analogue by addition of an excess of a strong base. The anionic PTM SAMs are oxidized to their PTM radical SAMs, either electrochemically or with a chemical oxidant.

To accomplish the three strategies, the synthesis of the two new PTM derivatives **3** and **4**, which incorporate a binding group to be anchored on gold, was carried out (Figure 1). Typically, thiol-functionalized molecules are employed to prepare SAMs on gold. However, PTM derivative **3** was designed bearing a thioacetyl group, which can also directly self-assemble on gold and is usually used to avoid the easy oxidation of thiols.[12] In the case of PTM diradical **4**, the binding group is a disulfide. It has also been proved that dialkyldisulfides on gold form SAMs identical to those of alkanethiols via cleavage of the S−S bond.[13]

Synthesis and Characterization of New PTM Derivatives. Thioacetyl triphenylmethane derivative **3** was synthesized by coupling under Wittig conditions 4-(acetylthio)benzaldehyde **1**[14] and the phosphonium salt **2**[15] (Scheme 2). By ^{1}H NMR and HPLC, it was proved that compound **3**, named also as αH-PTM-SAc, was obtained as the *trans* isomer.

Disulfide diradical **4** was prepared from derivative **3** in a one-pot reaction. First, **3** was treated with an excess of tetrabutylammonium hydroxide (TBAOH) in order to deprotect the thioacetate group to give the corresponding thiolate and at the same time to remove the acidic polychlorotriphenylmethane proton. The resulting carbanion derivative was not isolated but subsequently oxidized in situ to yield the diradical **4** using 2 equiv of solid $AgNO_3$ (Scheme 2). The thiolate group of the polychlorotriphenylmethide derivative is oxidized to the disulfide under the reaction conditions needed for the oxidation of the carbanion to the radical. Unfortunately, attempts carried out to obtain the anionic counterpart of **3** by using stoichiometric amounts of TBAOH failed.

UV–vis spectrum of **4** showed two bands at 386 nm (ϵ = 50073) and 575 nm (ϵ = 2739) that can be assigned to the radical character of the PTM unit, as well as an additional band at 444 nm (ϵ = 16188) which has been attributed to the electronic conjugation of the radical unit in the π-framework.[15] The formation of the diradical **4** was also proved by IR (KBr), where there is no presence of peaks at ca. 1600 cm^{-1} corresponding to the stretching of the carbonyl from the acetyl group. This confirmed that the deprotection of the thioacetyl took place successfully. The electron paramagnetic resonance (EPR) spectrum of diradical **4** was carried out in toluene/CH_2Cl_2 at 300 K (Figure 2). The spectrum showed three lines corresponding to the coupling of the two unpaired electrons with the two protons at the α position of the ethylene moiety as well as satellite lines that arise from the coupling with the aromatic carbons. Computer simulation of the EPR spectrum provides the *g* factor and the coupling constants (*a*). The *g* value is 2.0024, which is very similar to that observed for other PTM radicals.[16] The coupling constant with the proton atoms and with the carbon nuclei of the triphenylmethyl unit are a_H = 0.95 G, $a_1(^{13}C_\alpha)$ = 15 G, and $a_2(^{13}C_{arom})$ = 5.5 and 4.6 G, which are nearly half of those obtained for other substituted PTM monoradicals with similar side groups.[15,17] This occurs when

(8) Crivillers, N.; Mas-Torrent, M.; Perruchas, S.; Roques, N.; Vidal-Gancedo, J.; Veciana, J.; Rovira, C.; Basabe-Desmonts, L.; Ravoo, B. J.; Crego-Calama, M.; Reinhoudt, D. N. *Angew. Chem., Int. Ed.* **2007**, *46*, 2215–2219.
(9) (a) Matsushita, M. M.; Ozaki, N.; Sugawara, T.; Nakamura, F.; Hara, M. *Chem. Lett.* **2002**, *6*, 596–597. (b) Kashiwagi, Y.; Uchyama, K.; Kurashima, F.; Anazi, J.; Osa, T. *Anal. Sci.* **1999**, *15*, 907–909. (c) Mannini, M.; Sorace, L.; Gorini, L.; Piras, F. M.; Caneschi, A.; Magnani, A.; Menichetti, S.; Gatteschi, D. *Langmuir* **2007**, *23*, 2389–2397.
(10) Ballester, M.; Riera, J.; Castañer, J.; Badia, C.; Monsó, J. M. *J. Am. Chem. Soc.* **1971**, *93*, 2215–2225.
(11) (a) Sporer, C.; Ratera, I.; Ruiz-Molina, D.; Vidal-Gancedo, J.; Wurst, K.; Jaitner, P.; Rovira, C.; Veciana, J. *J. Phys. Chem. Solids* **2004**, *65*, 753–758. (b) Sporer, C.; Ratera, I.; Ruiz-Molina, D.; Zhao, Y.; Vidal-Gancedo, J.; Wurst, K.; Jaitner, P.; Cáliz, K.; Persoons, A.; Rovira, C.; Veciana, J. *Angew. Chem., Int. Ed.* **2004**, *43*, 5266–5268.
(12) (a) Tour, J. M.; Jones, L.; Pearson, D. L.; Lamba, J. J. S.; Burgin, T. P.; Whitesides, G. M.; Allara, D. L.; Parikh, A. N.; Atre, S. V. *J. Am. Chem. Soc.* **1995**, *117*, 9529–9534. (b) Kang, Y.; Won, D.-J.; Kim, S. R.; Seo, K.; Choi, H.-S.; Lee, G.; Noh, Z.; Lee, T. S.; Lee, C. *Mater. Sci. Eng.* **2004**, *24*, 43–46.
(13) (a) Biebuyck, H. A.; Bain, C. D.; Whitesides, G. M. *Langmuir* **1994**, *10*, 1825–1831. (b) Nuzzo, R. G.; Zegarski, B. R.; Dubois, L. H. *J. Am. Chem. Soc.* **1987**, *109*, 733–740. (c) Bain, C. D.; Biebuyck, H. A.; Whitesides, G. M. *Langmuir* **1989**, *5*, 723–727. (d) Noh, J.; Murase, T.; Nakajima, K.; Lee, H.; Hara, M. *J. Phys. Chem. B* **2000**, *104*, 7411–7416. (e) Grönbeck, H.; Curioni, A.; Andreoni, W. *J. Am. Chem. Soc.* **2000**, *122*, 3839–3842.
(14) Gryko, D. T.; Clausen, C.; Lindsey, J. S. *J. Org. Chem.* **1999**, *64*, 8635–8647.
(15) Rovira, C.; Ruiz-Molina, D.; Elsner, O.; Vidal-Gancedo, J.; Bonvoisin, J.; Launay, J.-P.; Veciana, J. *Chem.—Eur. J.* **2001**, *7*, 240–250.

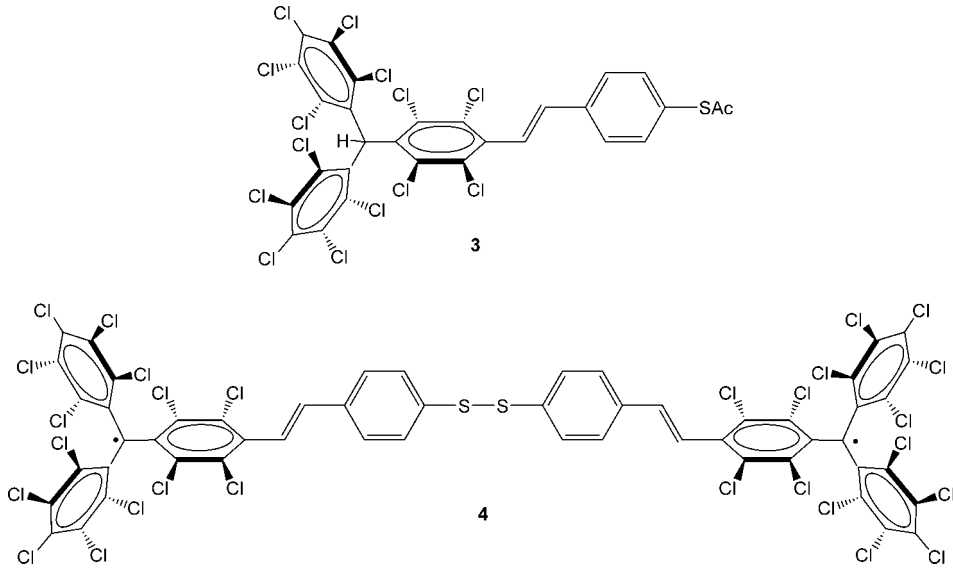

Figure 1. Molecular formula of the two new PTM derivatives used for the preparation of SAMs.

Scheme 2. Synthesis of PTM Derivative **3** and PTM Diradical **4**

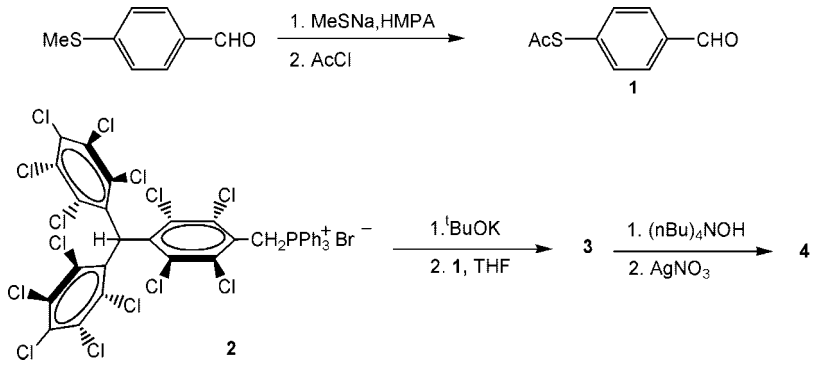

the two unpaired electrons in a diradical magnetically interact with a magnetic exchange coupling constant J that fulfils the following condition $J >> a_i$.[17] The obtained coupling constant values for compound **4** confirm its diradical character. Cyclic voltammetry of diradical **4** was also recorded in CH_2Cl_2 with 0.1 M NBu_4PF_6 as supporting electrolyte and using a Pt wire as a working electrode. The cyclic voltammogram shows a reversible redox wave with a reduction peak at −204 mV and an oxidation peak at −116 mV (vs Ag/AgCl), which are characteristic of PTM radicals.[17]

Preparation and Characterization of PTM SAMs. The preparation of SAMs on Au(111) derived from diradical **4** and the αH-PTM-SAc derivative **3** (Scheme 3) was achieved following the same methodology. A freshly cleaned gold substrate was immersed in a 0.1 mM THF solution of the corresponding compound under argon atmosphere. For αH-PTM-SAc **3**, gold substrates were immersed for approximately 24 h, whereas for PTM **4**, an immersion time of at least 72 h was required in order to have a high surface coverage. After this time, the monolayers were vigorously rinsed with abundant THF, to ensure that there was no physisorbed material on the substrate, and dried under N_2 stream. The resulting SAMs were characterized by contact angle, atomic force microscopy (AFM), and time-of-flight secondary ion mass spectroscopy (ToF-SIMS). The electrochemical and magnetic properties of these SAMs were investigated by cyclic voltammetry (CV) and EPR, respectively.

Contact angle values for the SAM of **4** and **3** were 80.0 ± 2.0° and 83.0 ± 0.7°, respectively, showing the high hydrophobicity of the layer. These values are also in agreement with the values found for PTM SAMs on silicon oxide.[8] Atomic force microscopy images also showed the formation of a highly homogeneous monolayer on the gold substrate (Supporting Information).

We have also used ToF-SIMS to characterize the SAMs that were prepared on gold substrates as well as on patterned gold surfaces. The methodology followed to prepare the patterned substrate is based on the microcontact printing technique[18] (see Experimental Section). ToF-SIMS is a highly sensitive and powerful surface characterization technique employed to determine the composition and structure of molecules on surfaces through mass spectral analysis.[19] There are several works

(16) (a) Ballester, J.; Riera, J.; Castañer, A.; Rodríguez, A. *Tetrahedron Lett.* **1971**, 2079. (b) Ballester, M.; Castañner, J.; Riera, J.; Ibañez, A.; Pujades, J. *J. Org. Chem.* **1982**, *47*, 259–264. (c) Ballester, M. *Acc. Chem. Res.* **1985**, *18*, 380–387. (d) Ballester, M.; Riera, J.; Castañer, J.; Rodriguez, A.; Rovira, C.; Veciana, J. *J. Org. Chem.* **1982**, *47*, 4498–4505. (e) Armet, O.; Veciana, J.; Rovira, C.; Riera, J.; Castañer, J.; Molins, E.; Rius, J.; Miravitlles, C.; Olivella, S.; Brichfeus, J. *J. Phys. Chem.* **1987**, *91*, 5608–5616.

(17) Lloveras, V.; Vidal-Gancedo, J.; Ruiz-Molina, D.; Figueira-Duarte, T. M.; Nierengarten, J.-F.; Veciana, J.; Rovira, C. *Faraday Discuss.* **2006**, *131*, 291–305.

(18) (a) Xia, Y. N.; Rogers, J. A.; Paul, K. E.; Whitesides, G. M. *Chem. Rev.* **1999**, *99*, 1823–1848. (b) Kumar, A.; Whitesides, G. M. *Appl. Phys. Lett.* **1993**, *63*, 2002–2004.

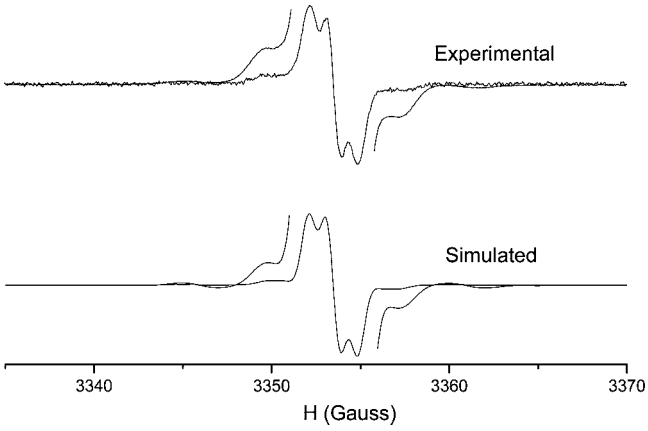

Figure 2. Experimental (top) and simulated (bottom) EPR spectra of diradical **4** in CH_2Cl_2/toluene recorded at 300 K.

Scheme 3. Scheme of the SAMs Based on PTM Derivatives **3** and **4** on Gold

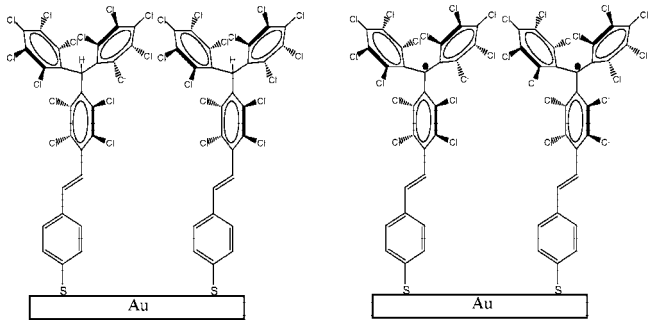

regarding the study of alkanethiol monolayers on gold by ToF-SIMS. The peak with mass corresponding to the AuM cluster (where M is the alkanethiolate molecule $C_nH_{2n+1}S^-$) along with the presence of molecular secondary ions such as $(AuSM)^-$ is often observed.[20]In our SAMs, the presence of chlorine atoms in the PTM-based molecules helps to assign and interpret their mass spectra since the appearing ion must show the isotopic distribution of chlorine atom ^{35}Cl (75.77%) and ^{37}Cl (24.23%) depending on the number of Cl atoms on each ion. Negative ToF-SIMS spectra were recorded for SAMs derived from **3** and **4**. In the mass region spectra of the SAM of **4** plotted in Figure 3, we observe two peaks at 1081 and 1113 *m/z*, which have the isotopic distribution corresponding to 14 chlorine atoms and, thus, can be undoubtedly assigned to PTM molecular fragments. We assign the peak at higher mass to $(MAuS_2)^-$ and the peak at lower mass to the cluster $(MAuS)^-$, with M = $C_{27}H_6Cl_{14}S$. The weak peak at 900 *m/z*, shown as the inset in Figure 3, might correspond to the formation of the sulfonate ion $(MO_3)^-$, probably due to the air oxidation of the SAM.[21] Similarly to the previous case, the ToF-SIMS spectra of compound **3** exhibited three peaks that clearly came from the PTM unit due to the fact that they displayed the characteristic isotopic chlorine distribution for 14 chlorine atoms. The ToF-SIMS spectrum of a SAM of **3** on a patterned gold substrate is shown in Figure 4. The right-hand image in this figure shows the ToF-SIMS image

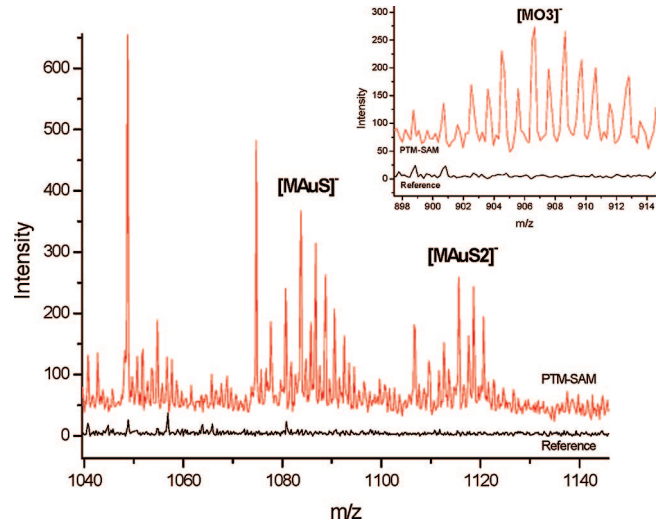

Figure 3. Negative-ion ToF-SIMS spectrum of the SAM of diradical **4**. Inset: peak at 900 *m/z* of this spectrum. The reference spectrum corresponds to bare gold.

corresponding to the peak at 1083 *m/z* (assigned to MAuSH), which proves that the PTM derivative is only present on the substrate regions covered by gold.

Cyclic voltammetry has been extensively used for the electrochemical characterization of self-assembled monolayers of electroactive molecules. Several works related on the study of the electron transfer rate in mixed SAMs prepared with ferrocene-containing thiols and *n*-alkanethiols have been carried out.[22] This technique was thus employed here to characterize the redox properties of the electroactive monolayer of SAMs of PTM diradical **4**. CV was carried out in CH_2Cl_2 and 0.1 M of tetrabutylammonium hexafluorophosphate as electrolyte (vs Ag/AgCl). The gold substrate functionalized with the SAM was used as a working electrode. In Figure 5, the cyclic voltammogram of this SAM is plotted, which shows one reversible redox wave with an oxidation peak at −192 mV and a reduction peak at −268 mV at a scan rate of 100 mV/s ($\Delta E = 76$). The stability of the SAM was elucidated by the reversibility of the process and the fact that after applying several redox cycles the response was unaltered. We also observed that increasing the scan rate resulted in an increase in the intensity of the peaks (Figure 5 inset), which is characteristic for surface-confined electroactive species. We also noticed a slight reduction of 12 mV in ΔE (i.e., voltage difference between the oxidation and reduction peaks), compared to the redox wave obtained for **4** in solution. This is an additional indication that the electroactive molecules are adsorbed on the surface. However, for an ideal situation in which electroactive centers are all close to the electrode surface and, therefore, diffusion should not have any influence in the process, and in which the surface-attached electroactive groups are noninteracting groups and in rapid equilibrium with the electrode, one would expect no splitting between the oxidation and reduction peaks.[23] Even though in our case we observed a very small reduction in ΔE, the separation between the two

(19) *ToF-SIMS: Surface Analisis by Mass Spèctrometry*; Vickerman, J. C., Briggs, D., Eds.; Surface IMP Publications; Chichester, U.K., 2001.
(20) (a) Tarlov, M. J.; Newman, J. G. *Langmuir* **1992**, *8*, 1398–1405. (b) Sohn, S.; Schröder, M.; Lipinsky, D.; Arlinghaus, H. F. *Surf. Interface Anal.* **2004**, *36*, 1222–1226.
(21) Li, Y.; Huang, J.; Hemminger, J. C. *J. Am. Chem. Soc.* **1992**, *114*, 2428–2432.
(22) (a) Chidsey, E. D.; Berozzi, C. R.; Putwinski, T. M.; Mujsce, A. M. *J. Am. Chem. Soc.* **1990**, *112*, 4301–4306. (b) Smalley, J. F.; Feldberg, S. W.; Chidsey, C. E. D.; Linford, M. R.; Newton, M. D.; Liu, Y.-P. *J. Phys. Chem.* **1995**, *99*, 13141–13149. (c) Sabapathy, R. C.; Bhattacharyya, S.; Leavy, M. C.; Cleland, W. E.; Hussey, C. L. *Langmuir* **1998**, *14*, 124–136. (d) Sekpr, S.; Misicka, A.; Bielwicz, R. *J. Phys. Chem. B* **2000**, *104*, 5399–5402. (e) Auletta, T.; Van Veggel, F. C. J. M; Reinhoudt, D. N. *Langmuir* **2002**, *18*, 1288–1293.

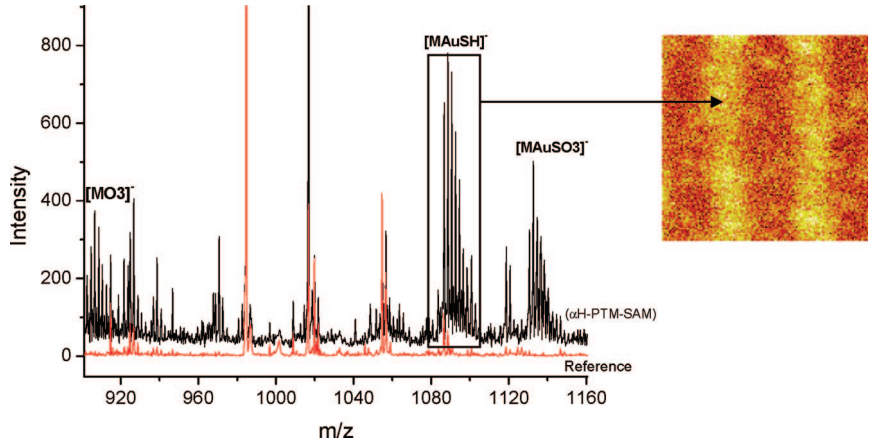

Figure 4. (Left) Negative-ion ToF-SIMS spectrum of the SAM of PTM **3**. The reference spectrum corresponds to bare gold, and the peaks at 985 and 1017 *m/z* in this spectrum are assigned to the gold clusters $[Au5]^-$ and $[Au5S]^-$, respectively. (Right) Negative ToF-SIMS image of the SAM of **3** on a patterned gold substrate (25 μm lines) at 1083 *m/z*.

potentials is considerable. Such peak splitting could be explained by the interaction between PTM moieties. One of the parameters that are used to indicate the interaction between redox centers is the full-width at half-maximum of the anodic (or cathodic) voltammetric wave, ΔE_{fwhm}. In the ideal situation, where there are no interactions between the redox centers, $\Delta E_{fwhm} = 3.53RT/nF$ (90.6 mV/n at 25 °C), where n is the number of electrons transferred in the process.[24] The deviations from this value have been attributed to the interaction between the redox centers. In the case of the SAM of PTM **4**, the ΔE_{fwhm} is 184 mV at a scan rate of 100 mV/s and, hence, points toward significant interactions between the PTM radicals. It is also worth mentioning that, at higher scan rates, the two redox peaks become more separated, up to 147 mV at 400 mV/s. This phenomenon may be rationalized in terms of the equilibrium at the surface, which at high scan rate might no longer be established due to a low electron transfer rate.[25] The surface area coverage can be determined by integration of the voltammetric wave current. From the anodic wave at 100 mV/s and considering that the area of the gold surface is 0.07 cm^2, we have estimated that the molecular coverage of the SAM of **4** is around 1.50×10^{14} molecules/cm^2. Considering this value, each PTM molecule would occupy an area approximately 0.67 nm^2, which is in agreement with the area estimated for one PTM molecule.[8] This demonstrates that the surface coverage in this SAM is extremely high.

On the other hand, although in the SAM of αH-PTM-SAc **3** the assembled molecules are non-electroactive, CV can be employed to demonstrate and evaluate the coverage of the SAM. This can be achieved considering the reductive desorption of the monolayer. The electrochemical desorption of thiol monolayers from gold is very well-known,[26] according to $AuSR + e^- \rightarrow Au^{(0)} + RS^-$. Figure 6 shows the cyclic voltammogram of the SAM of **3** in aqueous solution with 1 mM $K_3[Fe(CN)_6]$ and 0.1 M KCl. The functionalized gold substrate was used as a working electrode, and the CV response to the $[Fe(CN)_6]^{3-}/[Fe(CN)_6]^{4-}$ couple was used to investigate the efficiency of electrons transferring through the SAM. In the first CV scan, an almost flat line was recorded, which means that the surface is completely passivated by the non-electroactive molecular monolayer, and there is almost no transport of the $Fe(CN)_6^{3-}$ from the solution to the gold electrode. To induce the reductive desorption of this αH-PTM SAM, a series of cycles of negative voltages from −1.2 to −1.6 V at 100 mV/s were applied. As seen in Figure 6, the intensity of the redox peaks corresponding to the $[Fe(CN)_6]^{3-}/[Fe(CN)_6]^{4-}$ couple increased when more negative voltages were applied as a consequence of the SAM desorption. In the inset of Figure 6, the first and last CV scans are shown. For clarity, the first scan has been amplified 10×. Since we do not observe any further increase of the intensity of the peaks after applying more negative voltage cycles, we consider that the last scan corresponds to bare gold. Comparing these two redox waves, we observe that, in the first scan, (1) the oxidation and reduction peak currents are much lower, (2) there is less reversibility (i.e., wave less symmetric), and (3) the peak's separation (ΔE) is larger. These three experimental observations support the fact that, when the gold is modified with the non-electroactive αH-PTM-SAc molecules, the electron

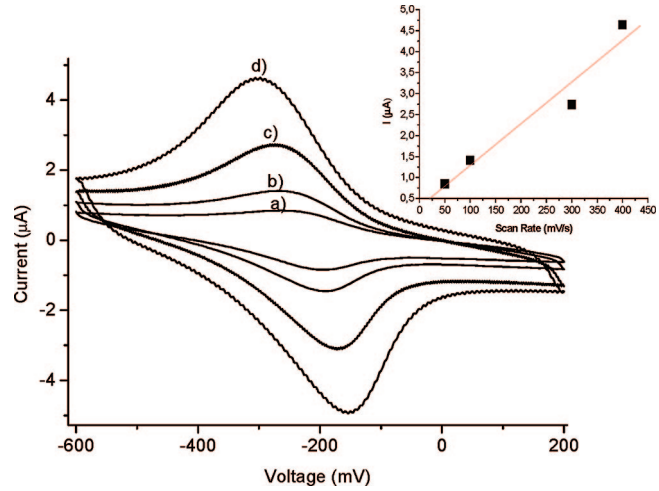

Figure 5. Cyclic voltammogram of the SAM of **4** in CH_2Cl_2, with 0.1 M n-Bu_4NPF_6 (vs Ag/AgCl) at different scan rates: (a) 50; (b) 100; (c) 300; and (d) 400 mV/s. Inset: Plot of the current intensity vs scan rate.

(23) Murry, R. W. In *Electroanalytical Chemistry*; Bard, A. J., Ed.; Marcel Dekker: New York, 1984; Vol *13*, pp 191–368 and references therein
(24) Bard, A. J.; Faulkner, L. R. *Electrochemical Methods: Fundamentals and Applications*; John Wiley & Sons: New York, 1980; p 522.
(25) Chidsey, C. E. D. *Science* **1991**, *251*, 919–922.
(26) (a) Widrig, C. A.; Cheng, C.; Porter, M. D. *J. Electroanal. Chem.* **1991**, *310*, 335–359. (b) Walczak, M. M.; Popenoe, D. D.; Deinhammer, R. S.; Lamp, B. D.; Chung, C.; Porter, M. D. *Langmuir* **1991**, *7*, 2687–2693. (c) Weisshaar, D. E.; Lamp, B. D.; Porter, M. D. *J. Am. Chem. Soc.* **1992**, *114*, 5860–5862.

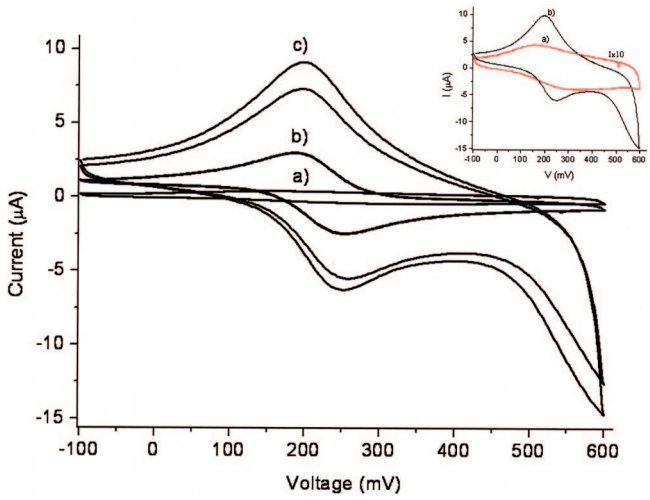

Figure 6. Cyclic voltammogram of the SAM of **3** in 1 mM $K_3[Fe(CN)_6]$ and 0.1 M KCl (electrolyte) vs Ag/AgCl. (a) Gold electrode passivated by PTM SAM (b and c) after applying cycles of negative voltage (from −1.2 to −1.6 V) for 20 scans (100 mV/s) and 40 scans, respectively. Inset: Cyclic voltammogram of the SAM of **3**, (a) first scan, amplified by 10×, (b) last scan, after that no increase of current intensity coming from the redox couple ($[Fe(CN)_6]^{3-}$/$[Fe(CN)_6]^{4-}$) was observed.

transfer is almost negligible,[27] which implies that the SAM derived from **3** has been successfully formed. Considering, as previously mentioned, the last CV plot as a bare gold electrode, we used the method reported by Weisser et al.[28] to calculate the hindrance (B) of the electrode, which is described by the following equation: $B = 1 - [i_p^{ox}(PTM)/i_p^{ox}(Au)]$. For our system, we obtained a value of 0.95. Although we should bear in mind that B is a qualitative value for the layer density, the results found point toward the formation of an almost full coverage layer.

Chemical reactions on the surface of PTM SAMs were also performed, allowing switching from the non-electroactive monolayer, the SAM of αH-PTM-SAc **3**, to an electroactive surface due to the generation of the anionic PTM species (see *Path b* in Scheme 1). A full coverage SAM of **3** was immersed in a 2 mM solution of tetrabutylammonium hydroxide in THF for 24 h under stirring and argon atmosphere. Then, the substrate was removed from the solution and washed with abundant THF. CVs were recorded before and after the deprotonation process. As it is shown in Figure 7a, no redox process takes place with the SAM formed with the protonated precursor **3**, while after the generation of the anionic PTM species in the SAM, oxidation and reduction peaks at −137 and −194 mV, respectively, are observed at 400 mV/s. The origin of the shifting of the redox process to higher voltage values compared to the SAM prepared from the PTM radical is still unclear, but it could be caused by the influence of the countercations adsorbed on the SAM. It should also be noticed that in this case the splitting between the oxidation and reduction peaks is smaller ($\Delta E = 57$ mV), which we attribute to lower interaction between the redox centers due to the formation of a less dense SAM (i.e., during the reaction conditions, there might be some desorption of the PTM molecules) and the fact that the tetrabutylammonium cations compensate the electrostatic repulsion.

The preparation of the electroactive SAM based on the anionic species derived from **3** was also achieved by forming the SAM directly from the anion (*Path c* in Scheme 1). To a 1 mM solution of **3** was added an excess of tetrabutylammonium hydroxide, and after stirring for a few seconds, the gold substrate was immersed for 24 h. Additionally, it is well-known that this basic treatment results also in the deprotection of the acetate group.[12a,29] The CV of the resulting SAM exhibited very similar redox potential values to the previous experiment (i.e., SAM of the anion formed in situ on the substrate), giving rise to one oxidation peak at −140 mV and a reduction peak at −190 mV (Figure 7b). However, AFM images showed the formation of a non-homogeneous layer, with the presence of very few small aggregates (4 nm height) that we ascribe to the perturbation of the monolayer by the presence of the bulky counterion from the base used.

The preparation of SAMs from the PTM anion derived from **3** has been performed following two different strategies showing very similar results. Also, the possibility to perform chemical reactions on PTM-functionalized surfaces has been demonstrated. However, as the CV results prove the method of preparing the SAMs directly from the electroactive PTM radical is more efficient since it requires less reactants and results in higher surface coverage.

Considering all results reported above, we demonstrated that PTM SAMs can be reversibly electrochemically interconverted to the radical and anion species. However, as stated before, in order to potentially apply these materials as switches, it is imperative to make use of a property that differs in both, the initial and final, states and use it as a read-out mechanism. In the present case, magnetic properties can be employed to read-out the state of the switch since, while PTM radicals are paramagnetic centers, the PTM anions are diamagnetic. To demonstrate the presence of paramagnetic species on the substrate, we performed electron paramagnetic resonance spectra on the SAMs in the two switchable states. The EPR spectrum of the SAM of diradical **4** on a surface area of 66 mm^2 was recorded at 300 K (Figure 8). A signal with a g value and a line width of 2.0026 and 4.1 Gauss, respectively, was observed, which is in accordance with the ones expected for an immobilized PTM radical. To prove the stability of the organic radical monolayer, several EPR spectra were registered, without any modification of the experimental parameters, during 2 weeks, and no noticeable changes were found. Importantly, from the EPR experiments, we can affirm that the radical behavior of PTM molecules is maintained when molecules are chemisorbed on a gold substrate.

The EPR spectra of the PTM anion formed following *Path c* was also recorded. As expected, no signal was observed due to its diamagnetic character. We can therefore conclude that the magnetic response can be employed to read the redox state of the SAM.

Summary

In summary, three different strategies have been followed in order to functionalize gold substrates with electroactive PTM derivatives. To achieve this goal, we have synthesized two new PTM derivatives with adequate S-based binding groups to be anchored on gold. SAMs based on these compounds have been prepared and fully characterized. The electrochemical charac-

(27) Weisser, M.; Nelles, G.; Wohlfart, P.; Wenz, G.; Mittler-Neher, S. *J. Phys. Chem.* **1996**, *100*, 17893–17900.
(28) (a) Weisser, M.; Nelles, G.; Wohlfart, P.; Wenz, g.; Mittler-Neher, S. *J. Phys. Chem.* **1996**, *100*, 17893–17900. (b) Bollo, S.; Yáñez, C.; Sturm, J.; Núñez-Vergara, L.; Squella, J. A. *Langmuir* **2003**, *19*, 3365–3370.
(29) Shaporenko, A.; Elbing, M.; Blaszcyk, A.; von Hänisch, C.; Mayor, M.; Zharnikov, M. *J. Phys. Chem. B* **2006**, *110*, 4307–4317.

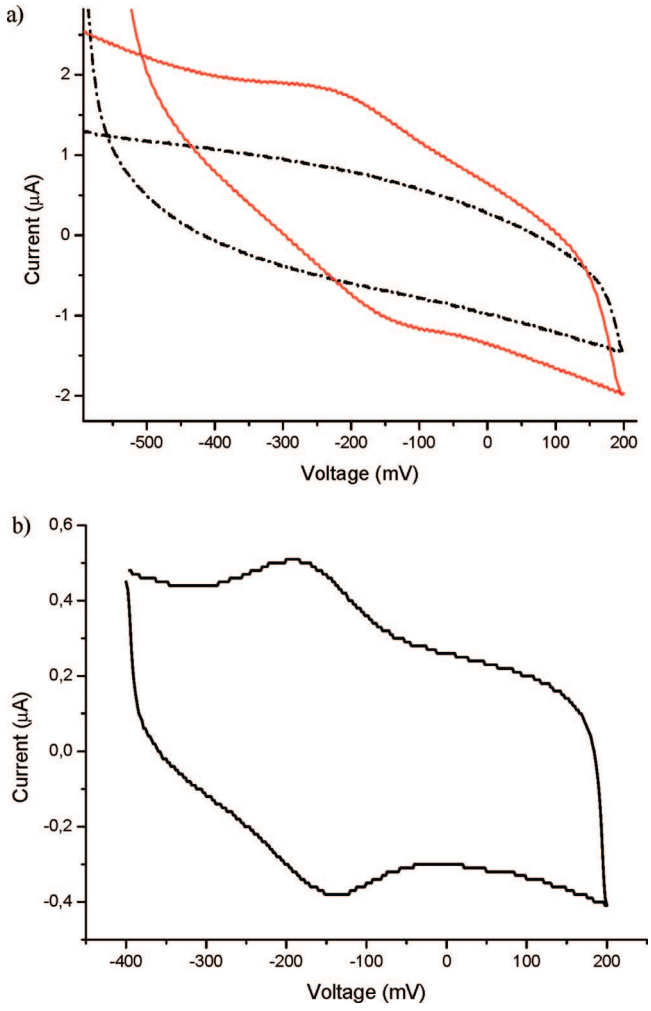

Figure 7. (a) Cyclic voltammogram of the SAM of **3** before (dashed line) and after (continuous line) deprotonation. (b) Cyclic voltammogram of the PTM anion SAM generated following *Path c*. All of these experiments were performed in CH_2Cl_2, with *n*-Bu_4NPF_6 (0.1 M) as supporting electrolyte (vs Ag/AgCl) and at a scan rate of 400 (a) and 100 mV/s (b).

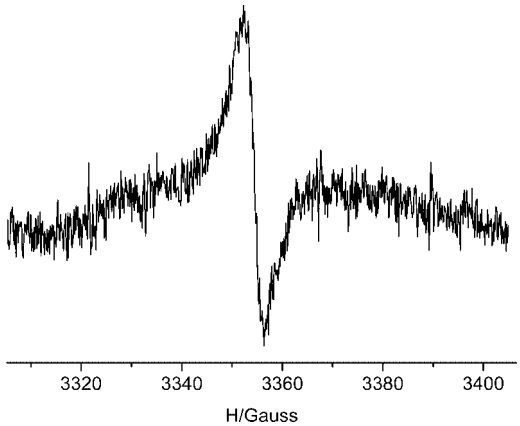

Figure 8. EPR spectrum of the SAM of **4** on gold, recorded at 300 K.

terization of the SAMs showed their high stability and large surface coverage. In addition, CV experiments demonstrated that it is possible to reversibly switch the PTM anchored to the Au surface from the radical state to its corresponding anion. Furthermore, the magnetic character of the surfaces functionalized with PTM radicals was proved by EPR. Combination of the electrochemical and magnetic properties makes PTM SAMs very attractive for preparation of molecular-scale memory devices.

Experimental Section

A ToF-SIMS IV mass spectrometer (Ion-Tof GmbH, Münster, Germany) equipped with a bismuth cluster (Bi3) ion source was used for these experiments. The primary ions hit the surface of the sample with a kinetic energy of 25 keV and an incidence angle of 45°. The primary ion current, measured with a Faraday cup on the sample holder, is 0.2 pA for Bi3++ at 10 kHz. The primary ion dose is between 4.7×10^{11} ions/cm^2 and 10^{12} ions/cm^2. The secondary ions are extracted with an energy of 2 keV and are postaccelerated to 10 keV just before hitting the detector surface (single channel plate followed by a scintillator and a photomultiplier). A low-energy electron flood gun is activated to neutralize the surface during the analysis. The effective ion flight path is 2 m using a reflectron, and the mass resolution is greater than 8000 full-width at half-maximum (fwhm) at *m/z* 35 and 10 000 (fwhm) at *m/z* 795.7. The scan area is 125×125 μm (256×256 pixels).

UV–vis spectra were recorded on a Varian Cary 300 Bio Instrument in double-beam mode.

EPR spectra were obtained at room temperature using a Bruker ELEXYS E500 X-band spectrometer. A rectangular TE102 cavity was used for the measurements. The signal-to-noise ratio of spectra was increased by accumulation of scans using the F/F lock accessory to guarantee large field reproducibility. Precautions to avoid undesirable spectral distortions and line broadenings, such as those arising from microwave power saturation and magnetic field over modulation, were also taken into account to improve sensitivity.

Contact angle measurements were measured with Millipore water on a OCA 15 with SCA20 software (Dataphysics, Germany).

Electrochemical experiments were performed with a potensiostat/galvanostat 263a from EG&G Princeton Applied Research, by using a platinum wire as working electrode and Ag/AgCl electrode as reference electrode. Anhydrous CH_2Cl_2 was freshly distilled over P_2O_5 under nitrogen. Commercial tetrabutylammonium hexafluorophosphate (Fluka, electrochemical grade (99.0%)) was used as the supporting electrolyte. For the CV of the SAMs, the molecular functionalized gold substrate was used as a working electrode.

General Procedures. Gold substrates were purchased from Arrandee (200–300 nm of gold on 1–4 nm of chromium on glass). Gold(111) was prepared by butane flame annealing in air after cleaning the substrates with acetone, dichloromethane, ethanol (5 min each in ultrasonic bath), and then in a piranha solution (1:3 H_2O_2/H_2SO_4) for 4 min. After cleaning with piranha, the substrates were vigorously rinsed with MQ water and dried under N_2 stream.

SAM formation was carried out under light exclusion and under argon atmosphere.

Patterned gold substrate preparation for ToF-SIMS was achieved by using a polydimethylsiloxane (PDMS) stamp that was inked with a solution of 1-dodecanethiol in ethanol and placed in contact with a gold substrate. This alkanethiol-patterned substrate was then immersed in an etching solution of a 1:1 mixture of $K_4[Fe(CN)_6]$/$K_3[Fe(CN)_6]$ (129/1) and $KOH/Na_2S_2O_3$ (2.25/1), which removed all gold area free of thiol. After that, to remove the organic material, the substrate was cleaned with a piranha solution and it was exposed for 1 h in an ozone atmosphere.

4-(Acetylthio)benzaldehyde (**1**)[14] and 1-[bis(2,3,4,5,6-pentachlorophenyl)methyl]-2,3,5,6-tetrachlorobenzyl]-4-(methyltriphenylphosphonium) bromide (**2**)[15] were synthesized as previously reported.

Synthesis of 1-[Bis(2,3,4,5,6-pentachlorophenyl)methyl]-4-[2-(4-acetylthiophenyl)etenyl]-2,3,5,6-tetraclorobenzene. Under dry conditions, 0.22 g (1.93 mmol) of potassium-*tert*-butoxide was added to a suspension of the phosphonium bromide salt **2** (1.92 g, 1.76 mmol) in 35 mL of dry THF at −78 °C. The mixture was stirred for 15 min, and then the cooling bath was removed. After 30 min, an orange ylide suspension was obtained. Then, 0.63 g (3.51 mmol) of 4-(acetylthio)benzaldehyde (**1**), dissolved in THF,

was added dropwise, and the resulting mixture was stirred for 72 h under argon atmosphere. Then, 30 mL of 1 N HCl was added. The crude product was extracted with two portions of 50 mL of $CHCl_3$, and the organic layer was washed four times with 50 mL of water, dried over Na_2SO_4, and evaporated under reduced pressure. Finally, chromatographic purification with silica and hexane/CH_2Cl_2 (75/25) yielded 1.025 g (65%) of **3** (white powder): ^{1}H RMN (*trans*-**3**) (500 MHz, $CDCl_3$) δ (ppm) 7.6 (d, J = 8.5 Hz, 2H), 7.48 (d, J = 8.5 Hz, 2H), 7.13 (d, J = 17 Hz, 1H), 7.09 (d, J = 17 Hz, 1H), 7.06 (s, 1H), 2.48 (s, 3H); FT-IR (KBr) υ_{max} (cm^{-1}) 3032, 2951, 2924, 2851, 1712, 1636, 1532, 1493, 1406, 1368, 1351, 1338, 1297, 1240, 1139, 1118, 1088, 1115, 969, 943, 871, 807, 718, 688, 668, 648, 613, 536, 528, 507, 484; MALDI-TOF (negative mode) ($C_{29}Cl_{14}H_{10}SO$, M = 902.8); (m/z) [M] = 902.08; [M − 43] = 859.08; [M − 70] = 832.08.

Synthesis of Diradical 1,1′-Bis(phenylethenyl)bis[(2,3,5,6-(tetrachlorophenyl)bis(pentachloropheyl)]methyl disulfide. An excess of tetrabutylammonium hydroxide (40% in water) was added to a solution of **3** (0.069 g, 0.076 mmol) in 35 mL of dry THF under argon atmosphere and under light exclusion. The resulting violet mixture was stirred for 6 h. To eliminate the excess of base, 30 mL of hexane and 30 mL of water were added to the solution. The organic phase was evaporated under reduced pressure, redissolved in CH_2Cl_2, and, after addition of hexane, gave a violet microcrystalline powder. The obtained compound was immediately stirred with 0.017 g (0.08 mmol) of $AgNO_3$ in 13 mL of dry CH_2Cl_2 for 2 h and 30 min at room temperature, under argon atmosphere and under light exclusion. After this time, the mixture was filtered off to eliminate Ag(0) formed. The solution was evaporated under pressure. The obtained compound was filtered on silica gel with hexane/CH_2Cl_2 (1/1). A dark green microcrystalline powder was obtained (14.27 mg, yield 22%): IR (KBr) υ_{max} (cm^{-1}) 2918, 1457, 1384, 1336, 1260, 1155, 1050, 963, 872, 817, 713, 652, 524; MALDI-TOF (m/z) (negative mode) ($C_{56}Cl_{22}H_{14}S_2$, M = 1719.6); (m/z) [M/2] = 859, [M/2 – 70] = 789; UV–vis (THF) [λ_{max}, (ϵ)] 386 nm (50073) and 444 nm (16188), 575 nm (2739); electrochemistry [CH_2Cl_2, Ag/AgCl] $E_{oxidation}$ = −116 mV, $E_{reduction}$ = −204 mV.

Acknowledgment. The authors thank H. Thomas, D. Maspoch, D. Ruiz-Molina, and C. Sporer for useful discussions. This work was funded by the European Science Foundation, EUROCORES FUNSmarts II project, and by the European project SURMOF (NMP4-CT-2006-032109), and was also supported by funds from the DGI, Spain (Project EMOCIONa, CTQ2006-06333/BQU), the Instituto Carlos III, MSyC, through "Acciones CIBER", and the EC Sixth Framework Programme Magmanet NoE (Contract no. 515767-2). N.C. thanks the Ministerio de Ciencia y Tecnología for a Ph.D. fellowship.

Supporting Information Available: AFM images of the αH-PTM-SAc SAM on Au(111). This material is available free of charge via the Internet at http://pubs.acs.org.

JA710845V